Conf-730823--10

LA-UR-73-981

IAEA-SM-174/74

# DYNAMICS OF FISSION AND FUSION

# WITH APPLICATIONS TO THE FORMATION OF SUPERHEAVY NUCLEI

by

A. J. Sierk and J. R. Nix

August 1, 1973

For presentation at the Third IAEA Symposium on the
Physics and Chemistry of Fission,
Rochester, New York, August 13-17, 1973



los alamos
scientific laboratory
of the University of California
LOS ALAMOS, NEW MEXICO 87544



UNITED STATES
ATOMIC ENERGY COMMISSION
CONTRACT W-7405-ENG. 36

# DYNAMICS OF FISSION AND FUSION WITH APPLICATIONS TO THE FORMATION OF SUPERHEAVY NUCLEI*

A. J. SIERK and J. R. NIX
Los Alamos Scientific Laboratory, University of California
Los Alamos, New Mexico, United States of America

## ABSTRACT

Within the framework of the liquid-drop model we study various aspects of the dynamical evolution of nuclei: the effects of viscosity on the separation of fission fragments, the fission of very large nuclei, and the fusion of two heavy ions. The effect of viscosity on the post-scission motion of fission fragments is calculated by assuming an irrotational flow pattern in spheroidal fragments. As the viscosity increases from 0 to $\infty$, the fission fragments remain prolate for a longer time, which increases the post-scission fragment kinetic energy. This increase is about 13 MeV for the symmetric fission of $^{236}$U.

We calculate the dynamical path from an initially spherical configuration to scission for nuclei with fissility parameter x between 1.0 and 1.6 by use of the three-quadratic-surface shape parametrization. The inertias are calculated by means of the Werner-Wheeler approximation for irrotational flow. The motion is assumed nondissipative. As the Coulomb energy increases, the scission configuration becomes more and more elongated. As a specific example, we calculate the evolution of an initially spherical $^{476}$184 nucleus, formed from two $^{238}$U nuclei. It has been suggested that this system might form a superheavy nucleus by asymmetric fission. At scission the calculated length of this nucleus is about 14 times the diameter of the initial sphere. This result indicates that the nucleus would probably fission into three or more fragments if this were allowed by the shape parametrization. To complement this calculation, we compute the static potential energy of two tangent spheroidal fragments of the $^{476}$184 nucleus corresponding to $^{300}$116 and $^{176}$Er. Configurations stable against fission of the $^{300}$116 nucleus have an energy over 100 MeV higher than the minimum energy of two tangent spheroids and the energy of the scission point in the dynamical calculation. Single-particle effects lead to a small local minimum in the potential energy near the spherical heavy fragment with a barrier

---

* This work was performed under the auspices of the United States Atomic Energy Commission.

of about 4 MeV against prolate distortions. We conclude from these results that the fusion-fission reaction of very heavy ions is not likely to produce superheavy nuclei.

We study the fusion reactions of two initially spherical tangent nuclei at various incident energies above the interaction-barrier height. These calculations also do not contain viscosity and use the same shape parametrization as the fission study. This parametrization is deficient in that for most cases we are unable to follow the evolution to the point where the nuclei refission. We calculate as a function of fissility parameter $x$ the amount of incident energy necessary for symmetric systems to fuse to a configuration more compact than the liquid-drop-model saddle-point shape. As specific examples we consider the symmetric reactions $^{110}Pd + ^{110}Pd$ and $^{238}U + ^{238}U$.

## 1. INTRODUCTION

We have already seen in this symposium that dynamics plays an important role in many phenomena in fission and heavy-ion reactions. These include the division of the total energy released in fission into fission-fragment kinetic energy and internal excitation energy, and the amount of incident kinetic energy needed to cause fusion in a heavy-ion reaction.

The most fundamental way to study nuclear dynamics is of course to use a microscopic approach, as discussed earlier by Pauli [1] and others. However, because of the large amount of computing that is required, it is not yet feasible with such approaches to solve the equations of motion for the time evolution of the system. We therefore use a much simpler macroscopic approach, where the dynamics is treated in terms of classical hydrodynamical flow. Previous studies of this type [2-4] have been limited primarily to nonviscous irrotational flow and have been applied only to the fissio of nuclei with fissility parameter $x$ less than 1.0. (The fissility parameter is defined as the ratio of the Coulomb energy of a spherical sharp-surface drop to twice the spherical surface energy.) Natural extensions of this earlier work include the introduction of nuclear viscosity, the fission of heavier nuclei, and the study of fusion reactions. Certain aspects of these three extensions are considered in Secs. 2, 3, and 4, respectively.

In calculating the potential energy of the system, we include only the surface and Coulomb energies of the liquid-drop model. Although single-particle corrections to the potential energy are important in many specific phenomena, they have a small influence on the average trends of dynamical effects over the broad region of nuclei that we are considering. The equations of motion are solved classically because the DeBroglie wavelength of the motion is usually much smaller than distances over which the potential energy changes by an appreciable amount. Furthermore, we do not yet know how to incorporate dissipative effects into a quantum-mechanical equation of motion.

For small deformations, corresponding to the ground state and the region of the fission barrier, we know that the true nuclear inertia is several times the value corresponding to classical hydrodynamical flow, and in this region the treatment of nuclear dynamics in terms of classical hydrodynamical flow is seriously deficient. However, for larger distortions, such as those in the later stages of fission or near the point of first touching in heavy-ion reactions, experimental values for inertias are poorly

known, and values calculated by use of the cranking model are close to the irrotational-flow values. This suggests that a classical hydrodynamical treatment may be sufficiently accurate for these larger distortions.

There are two general methods for computing hydrodynamical flow. One method is to solve the complete Navier-Stokes equations for a viscous fluid by means of finite-difference numerical techniques. A faster but more limited approach is to describe a nuclear shape by a small number of coordinates and to follow the time evolution of these coordinates. There have been some attempts in nuclear physics to use the first method but no results have appeared yet. We choose the second method because of its relative simplicity.

Because we are interested in both fission and fusion reactions, we choose a shape parametrization that describes shapes occurring in both processes. The shapes are restricted to axial symmetry and are formed by connecting smoothly two end spheroids with a central quadratic surface, which may be either a spheroid or a hyperboloid of revolution. This parametrization contains three symmetric and two asymmetric degrees of freedom, but is limited by not being able to describe either multi-fragment fission or many shapes encountered in heavy-ion fusion. However, even with these restrictions, we are able to learn several interesting properties of fission and fusion reactions.

## 2. EFFECTS OF VISCOSITY ON THE SEPARATION OF FISSION FRAGMENTS

One of our primary objectives is to study the effect of viscosity on nuclear dynamics. We introduce viscosity by means of the Rayleigh dissipation function

$$\mathcal{F} = \frac{1}{2} \sum_{i,j} \eta_{ij}(\vec{q})\, \dot{q}_i\, \dot{q}_j \quad ,$$

where $\dot{q}_i$ is the time derivative of the shape coordinate $q_i$ and where $\eta_{ij}$ is an element of the viscosity tensor. The viscosity tensor, which is a function of the nuclear shape, is calculated by equating $\mathcal{F}$ to one-half the rate of energy dissipation from collective modes to internal energy. The equations of motion become the generalized Lagrange equations

$$\frac{d}{dt}\left(\frac{\partial \mathcal{L}}{\partial \dot{q}_i}\right) = \frac{\partial \mathcal{L}}{\partial q_i} - \frac{\partial \mathcal{F}}{\partial \dot{q}_i} \quad ,$$

where the Lagrangian $\mathcal{L} = T - V$ is also a function of $q_i$ and $\dot{q}_i$. The kinetic energy is T, and V is the potential energy. The introduction of viscosity adds to the equations of motion terms linear in the first time derivatives of $\vec{q}$. Most of the inertial effects are included in terms containing second time derivatives of $\vec{q}$, while the generalized forces are described primarily by terms involving the zeroth time derivative of $\vec{q}$.

Eventually we plan to solve the equations of motion with viscosity included for the descent from the saddle point to scission. Then by comparing the calculated most probable fission-fragment kinetic energies with experimental values, we should be able to deduce an average value for the coefficient of nuclear viscosity appropriate to large distortions, which is poorly known at present [5].

We have not yet computed $\mathcal{T}$ for our full parametrization but have studied instead the separation of two viscous fission fragments constrained to spheroidal shapes. Although we are able to treat a more general case (unequal fragments rotating in a plane formed by their symmetry axes), we present here results corresponding to the separation of equal collinear fragments. In this case the coordinates of interest are the center-of-mass separation $r$ and the semi-symmetry axis $c$ of the spheroids. The fragments are taken to be initially at rest in the configuration of tangent spheroids of minimum potential energy. The inertia and viscosity tensors are calculated by assuming incompressible, irrotational hydrodynamical flow. This approximation is discussed in the appendix.

The equations of motion for the symmetric spheroids are

$$\dot{p}_r = -\frac{\partial V}{\partial r}$$

and

$$\dot{p}_c = -\frac{\partial V}{\partial c} + \frac{p_c^{\,2}}{2M_c^{\,2}}\frac{dM_c}{dc} - \frac{4\pi R_0^{\,3}\mu \dot{p}_c}{M_c\, c^2} \quad ,$$

where the two conjugate momenta are $p_r = M_r\,\dot{r}$ and $p_c = M_c\,\dot{c}$ and where the two elements of the diagonal inertia tensor are

$$M_r = \frac{1}{4} M_0$$

and

$$M_c = \frac{1}{5} M_0 [1 + \frac{1}{4} (R_0/c)^3] \quad .$$

The quantity $M_0$ is the mass of the original spherical nucleus, $R_0$ is its radius, and $\mu$ is the coefficient of nuclear viscosity.

We show in Fig. 1 the center-of-mass separation $r$ and the fragment elongation $\sigma$ of two symmetric fragments resulting from the fission of a nucleus with fissility parameter $x = 0.7$. The points are given at equal time intervals for varying values of viscosity. The coordinates $r$ and $\sigma$ [6] are generalizations of $r$ and $c$ which are useful for the more complex shapes that we consider later. If we bisect a reflection-symmetric shape at its center and define $\langle f \rangle$ as the average value of the function $f$ over one-half the mass distribution, then $r = 2\langle z \rangle$ and $\sigma = (\langle z^2 \rangle - \langle z \rangle^2)^{\frac{1}{2}}$. For two separated spheroids, $\sigma$ is exactly $c/\sqrt{5}$.

In Figs. 1 and 2 the viscosity is given in terms of the natural unit [2,3]

$$\mu_0 = \left[M_0\, E_s^{(0)}\right]^{\frac{1}{2}} R_0^{-2} \quad .$$

When the second set of liquid-drop-model constants of Myers and Swiatecki [7] is used for a nucleus with fissility parameter $x = 0.7$ along Green's approximation to the line of beta stability [8], the resulting value is $\mu_0 = 6.73 \times 10^{17}$ MeV sec cm$^{-3}$ $= 1.08 \times 10^{12}$ gm cm$^{-1}$ sec$^{-1}$ (poise). It is worth noting that a direct comparison of the magnitude of nuclear viscosity with that of familiar macroscopic systems is misleading because of scaling effects.

The effect of viscosity on this system, as shown in Fig. 1, is qualitatively similar to that on a one-dimensional harmonic oscillator. For small values of viscosity, the shape oscillations continue with damped amplitude. As the viscosity increases to a critical value, the fragments approach spherical shape nearly exponentially. For very large values of viscosity the fragments approach the spherical shape much more slowly.

We show in Fig. 2 the change in post-scission kinetic energy relative to nondissipative motion for fragments with different amounts of viscosity. Because two prolate spheroids have a higher Coulomb interaction energy than two spheres with the same center-of-mass separation, the kinetic energy for very viscous fragments is larger than that for no dissipation. For small values of viscosity, the fragment energy is less than that for no viscosity because of the increased time the system spends with a significant oblate deformation relative to the time with a prolate shape.

## 3. FISSION OF VERY LARGE NUCLEI

Heavy-ion reactions that might produce superheavy nuclei lead to systems with fissility parameter $x$ greater than 1. It is therefore important to know the fission properties of such systems, which are already being produced in heavy-ion reactions.

We calculate the dynamical evolution of nuclei with $x$ greater than 1.0 by use of the three-quadratic-surface shape parametrization. The effective masses for irrotational flow are calculated by means of the Werner-Wheeler method, where the flow is approximated by circular layers of fluid which move along the symmetry axis and change their radii but do not lose their disk-like shape [2,3]. Viscosity is not included. The initial conditions correspond to starting at a spherical shape with zero kinetic energy (at $t = -\infty$). In Fig. 3 we show the division of the energy released in fission as a function of $x$. The energy is divided into translational kinetic energy (acquired before and after scission) and deformation energy of the fragments at infinite separation. The Coulomb forces cause an increase in deformation energy at scission for large values of $x$, with more than half of the energy release going into deformation energy for $x$ greater than 1.42. However, this large deformation energy is partly a result of our method of parametrizing the nuclear shape. Since we restrict the system to binary fission, it cannot reduce its large deformation energy by fissioning into three or more fragments.

As a specific example, we consider the $^{476}184$ system, which can be formed from the fusion of two $^{238}$U nuclei. We investigate this problem from two complementary points of view: the dynamical evolution of an initially spherical $^{476}184$ nucleus, and the static potential energy as a function of fragment deformation for two tangent spheroidal fission fragments from the same nucleus.

In Fig. 4 we present the sequence of shapes followed by an initially spherical $^{476}184$ nucleus with 1 MeV of energy in the fission degree of freedom at time intervals of $10^{-21}$ sec. The Coulomb forces cause a very large fragment elongation, to a maximum length of more than 14 times the initial diameter of the sphere. This fact suggests that multi-body fission would occur in a less restricted shape parametrization. The fission of a $^{236}$U nucleus, started from the liquid-drop-model saddle point with 1 MeV of

kinetic energy in the fission direction is also shown in Fig. 4 for comparison with the result for $^{476}184$. The inclusion of viscosity in these calculations could cause the results to change significantly. In particular, large viscosity might cause the fragments to be much less elongated at scission.

In Fig. 5 we show a potential-energy map for two tangent spheroids, where the coordinates are the ratios $c/a$ of the semi-symmetry to the semi-transverse axes for the two fragments. The energies are calculated by use of the droplet model [9], which contains primarily surface and Coulomb energies, but also includes higher-order corrections in $A^{-1/3}$ and $[(N-Z)/A]^2$ than are retained in the liquid-drop model; the constants are taken from the January 1973 analysis of Myers and Swiatecki [10]. The two fragments are taken to be $^{300}116$ and $^{176}$Er, a division which approximately conserves the charge density of the $^{476}184$ parent system. The minimum energy of the system with the heavy nucleus spherical corresponds to a light-fragment semi-axis ratio $c/a = 12.6$ and is 126 MeV higher than the absolute minimum-energy configuration. This latter configuration corresponds to a light-fragment semi-axis ratio $c/a = 2.1$ and a heavy-fragment semi-axis ratio $c/a = 11.9$. Both of these minima are artifacts of the spheroidal shapes chosen, as the fragments would undergo fission if allowed to form a neck.

In Fig. 6 we show the potential energy of the tangent spheroids as a function of deformation of the superheavy fragment with the light fragment held fixed at the semi-axis ratio $c/a = 12.6$. To the droplet energy we add the single-particle corrections calculated for the $^{300}116$ nucleus isolated from external interactions [11], which gives an estimate of the maximum effect of shell and pairing corrections. The single-particle effects lead to a local minimum in the potential energy, but the energy at this minimum is still more than 100 MeV higher than the energy of the configuration with the very elongated superheavy fragment and the energy of the scission configuration for the dynamical fission calculation described above. Because of this large energy difference, the probability for the large fragment to be formed with a semi-axis ratio less than the saddle-point value of 1.2 is extremely small.

In private discussions Vandenbosch has suggested that the presence of the Coulomb forces from the second fragment could possibly prevent the heavy fragment from undergoing fission by driving it toward a spherical shape. We estimate the importance of this effect by calculating the maximum elongation of the superheavy nucleus which could be driven to a spherical shape by a spherical light fragment initially in contact. This maximum elongation occurs at a semi-axis ratio for the $^{300}116$ fragment of $c/a = 2.0$. This value represents an upper limit because in this estimate the positions of the centers of mass of the fragments are held constant instead of being allowed to separate, and the light fragment is spherical instead of a more probable prolate spheroid.

We have shown that the production of superheavy nuclei from the asymmetric fission of nuclei with mass number $A \approx 500$ is highly improbable. This conclusion has been reached only for nonviscous motion; the result would be modified if very viscous flow resulted in fragment elongation at scission with a semi-axis ratio $c/a$ significantly less than 2.0. For viscous flow the value would need to be less than 2.0 because the large fragment would not be able to respond quickly to the Coulomb restoring force of the lighter fragment before the two nuclei separate.

## 4. FUSION OF HEAVY IONS

We use the shape parametrization described in Sec. 3 and the dynamical equations in Ref. [3] to study the fusion of two initially spherical nuclei with zero relative angular momentum. In Fig. 7 we show the evolution of two $^{110}$Pd nuclei interacting to form $^{220}$U at various energies above the liquid-drop interaction barrier. (All energies are in the center-of-mass system.) Two $^{238}$U nuclei are shown in Fig. 8 interacting at various energies to form a $^{476}$184 system. These two examples are qualitatively different: The $^{220}$U system has a fission barrier with a liquid-drop-model saddle-point energy of about 5 MeV and would thus form a compound system for a significant range of collision energies (for nonzero viscosity), whereas the $^{476}$184 nucleus is unstable with respect to small spheroidal distortions and therefore has no fission barrier. In comparing Figs. 7 and 8 with Fig. 4 we see that the time scale for fusion reactions is much shorter than for fission.

These figures show the limitations of our shape parametrization for describing fusion reactions. For low energies, after the spheres touch the surface energy causes a rapid filling-in of the neck, which results in a shape with flattened ends and a high surface energy. This surface energy and the Coulomb forces cause the end bodies to rapidly become prolate and to intersect in a manner that forms a cusp at the middle of the shape. The inclusion of viscosity may slow down the motion to a point where this phenomenon does not occur. The situation would also be improved by including the effects of the finite range of the nuclear force on the macroscopic energy (instead of representing the energy in terms of surface tension), as discussed in this symposium by Krappe [12]. This improvement would greatly reduce the rapidity with which the neck grows after first contact. For higher energies the fusion continues until the system approaches a pure spheroidal form. Shapes close to a spheroid are not handled adequately by our parametrization, and the integration terminates when this condition occurs. For even higher energies, the end-flattening of the system, which is apparent at lower energies, proceeds to the point where the ends attempt to become concave, a type of shape that is not describable in any parametrization of the form $\rho = \rho(z)$. This end-flattening is a result of the rapid growth of the neck; the assumption of incompressible and nearly irrotational fluid flow requires that the material filling the neck comes primarily from the ends of the body. We conclude that a complete investigation of fusion reactions requires an unconstrained shape description.

Even within these limitations imposed by our coordinates, we learn a significant amount from these calculations. In a two-dimensional space described by the coordinates defined in Sec. 2 for reflection symmetric shapes (center-of-mass separation and the second central moment of the fragment shape), we present in Fig. 9 the paths followed by two colliding $^{150}$Nd nuclei, which is a possible choice for producing the superheavy nucleus $^{300}$120 by a symmetric collision. We see that more than 100 MeV of energy over the interaction barrier (which is approximately 400 MeV high) is needed to drive the system to a nearly spherical shape, an indication of a lower limit to the additional energy required to produce a superheavy nucleus from such a collision, if such production is possible. Of course, for viscous flow even more energy would be required.

A recent paper by Lefort et al. [13] reports a very small probability for complete fusion when $^{209}$Bi nuclei are bombarded with $^{84}$Kr ions of

500-MeV energy, which is (35±9) MeV over the calculated interaction barrier in the center-of-mass system [12]. We have not yet calculated fusion reactions for such asymmetric systems, but some qualitative comparisons may be made. The $^{293}119$ system resulting from the above reaction is similar to the $^{300}120$ system considered in our symmetric dynamical calculation. For this calculation, more than 100 MeV of energy over the interaction barrier is required to bring the nuclei close enough for a long enough time to allow a significant mass transfer between the interacting nuclei. We expect the energy required for fusion to be somewhat less for an asymmetric system than for a symmetric one, but still of the same order of magnitude. The observed lack of fusion at the 35-MeV energy may be due either to the tendency of the nuclei to quickly re-fission because of the large Coulomb forces and the distribution of energy into degrees of freedom other than center-of-mass motion, as indicated in Fig. 9, or because large nuclear viscosity prevents mass transfer between the nuclei, or to a combination of these effects. The disruptive effect of angular momentum appears to be too small to account for the very small cross sections observed [13].

By use of plots similar to the one in Fig. 9 for different nuclei we find the minimum-energy collision whose trajectory passes inside the liquid-drop-model saddle point. This gives an estimate of the lower limit to the energy needed to cause a complete fusion. In Fig. 10 we show this critical energy as a function of the fissility parameter. For values of $x$ less than 0.72 no energy over the interaction barrier is needed. Above this value, the critical energy rises steeply to about $0.15\ E_s^{(0)}$, which is needed to reach the saddle-point shape for $x \approx 0.9$. For a nucleus along the line of beta stability, this energy is about 110 MeV above the interaction barrier. For larger values of $x$, we are not able to determine the critical energy because the calculated paths terminate before reaching the saddle point. This criterion of passing inside the liquid-drop-model saddle point is necessary but not sufficient to form a compound system. This is because a nonviscous system will ultimately re-fission since its total energy is higher than its saddle-point energy. Some dissipation must be present in order to form compound nuclei from heavy-ion reactions.

## 5. SUMMARY AND CONCLUSION

We have investigated several aspects of nuclear dynamics on the basis of the liquid-drop model, including the effect of viscosity on the separation of fission fragments, the fission of very large nuclei, and symmetric fusion reactions involving systems of different masses and interaction energies. We find that for small viscosities the often-suggested fusion-fission reaction method is highly unlikely to lead to the formation of superheavy nuclei. Although our nuclear shape parametrization has deficiencies for fusion reactions and the fission of large systems, it still provides some worthwhile information.

A major objective of this type of study is to calculate cross sections for fusion reactions. Ideally, one would like to do this by solving the full Navier-Stokes equations for unconstrained shapes, but even within our restricted shape parametrization there are three extensions to be made: the consideration of viscosity, the inclusion of angular momentum, and the calculation of the macroscopic energy by including the finite range of the nuclear force instead of by using surface tension. We are now in the process of calculating most-probable fission-fragment kinetic energies for viscous flow. By comparing these calculations with experimental results we

hope to deduce an average value for the coefficient of nuclear viscosity that is appropriate to large distortions. Once the coefficient of viscosity is known, it should be possible to estimate fusion cross sections for heavy systems by performing similar dynamical calculations with the inclusion of vicsocity, angular momentum, and the finite range of the nuclear force in the macroscopic energy.

---

## APPENDIX. EFFECT OF VISCOSITY ON THE INERTIA AND VISCOSITY TENSORS FOR THE SMALL OSCILLATIONS OF A CLASSICAL LIQUID DROP

The effect of viscosity on the inertia and viscosity tensors is computed from the exact solution to the Navier-Stokes equations for small motions about a spherical shape. For small values of viscosity the flow remains nearly irrotational, so irrotational flow gives a very good approximation to the correct inertia and viscosity tensors. The normal modes for nearly-spherical shapes for all values of viscosity are the quantities $\alpha_i$, where the surface of the axially symmetric drop is given by

$$R(\theta) = \frac{R_0}{\lambda}\left[1 + \sum_{i=2}^{\infty} \alpha_i(t)\, P_i(\cos\theta)\right] \quad .$$

The diagonal elements $\eta_{ii}$ of the viscosity tensor are monotonically increasing functions of the coefficient of viscosity $\mu$; the ratio $\eta_{ii}/\mu$ decreases from the irrotational flow value at $\mu = 0$ to a fraction of this number as $\mu \to \infty$. For the $i = 2$, 3, and 4 modes, respectively, the ratios $\eta_{ii}/\mu$ at infinite viscosity are 75%, 69%, and 63% of the values at $\mu = 0$. The elements of the inertia tensor are also monotonically increasing functions of $\mu$; the $i = 2$, 3, and 4 elements reach 105%, 111%, and 117% of their nonviscous values as $\mu \to \infty$. We see that the irrotational-flow values provide a good estimate for the inertia and viscosity tensors for the small oscillations of classical liquid drops. The fragment distortions considered in Sec. 2 are somewhat larger than the small oscillations studied here, but the inaccuracies introduced by the larger distortions are no larger er than those caused by viscosity. We re-emphasize that we are considering the effect of classical viscosity on the inertia and viscosity tensors, and not the potentially large changes caused by single-particle effects.

## REFERENCES


[1] PAULI, H. C., LEDERGERGER, T., Paper IAEA-SM-174/206, these Proceedings.
[2] NIX, J. R., SWIATECKI, W. J., Nucl. Phys. 71 (1965) 1.
[3] NIX, J. R., Nucl. Phys. A130 (1969) 241.
[4] HASSE, R. W., Nucl. Phys. A128 (1969) 609.
[5] WIECZOREK, R., HASSE, R. W., SÜSSMANN, G., Paper IAEA-SM-174/2, these Proceedings.
[6] KOONIN, S. E., private communication (1972).
[7] MYERS, W. D., SWIATECKI, W. J., Ark. Fys. 36 (1967) 343.
[8] GREEN, A. E. S., Nuclear Physics, McGraw-Hill, New York (1955) 185, 250.
[9] MYERS, W. D., SWIATECKI, W. J., Ann. Phys. 55 (1969) 395.
[10] MYERS, W. D., SWIATECKI, W. J., private communication (1973).
[11] BOLSTERLI, M., FISET, E. O., NIX, J. R., NORTON, J. L., Phys. Rev. C 5 (1972) 1050.
[12] KRAPPE, H. J., NIX, J. R., Paper IAEA-SM-174/12, these Proceedings.
[13] LEFORT, M., NGÔ, C., Péter, J., TAMAIN, B., Orsay Preprint IPNO-RC-73-06 (1973).

## FIGURE CAPTIONS

FIG. 1. Calculated fragment elongation $\sigma$ and center-of-mass separation $r$ for spheroidal fission fragments for a nucleus with fissility parameter $x = 0.7$. The coordinate $\sigma$ is $c/\sqrt{5}$, where $c$ is the semi-symmetry axis of the spheroidal fragments. The paths are plotted at equal time intervals of $0.4\ T_0 \approx 1.8 \times 10^{-22}$ sec for five values of the viscosity $\mu$. The natural unit of viscosity is $\mu_0 = [M_0 E_s^{(0)}]^{1/2} R_0^{-2}$. The shapes corresponding to selected values of these coordinates, indicated by the plus signs, are shown in the top part of the figure. The sloping lines give the configurations of two tangent spheroids, and the horizontal lines give the configurations of two separated spheres.

FIG. 2. Calculated change in fragment kinetic energy due to viscosity as a function of the fissility parameter $x$ for spheroidal fission fragments. The energy change is plotted as $[E(\mu) - E(0)]/E_s^{(0)}$ where $E_s^{(0)}$ is the surface energy of the original spherical nucleus. The natural unit of viscosity is $\mu_0 = [M_0\ E_s^{(0)}]^{1/2} R_0^{-2}$.

FIG. 3. Calculated division of the energy in fission for idealized nonviscous nuclei as a function of the fissility parameter $x$. The total energy available is the sum of the energy release $E_{rel}$ and the fission-barrier height $B_f$. This energy is divided into prescission translational kinetic energy, post-scission translational energy, and fragment vibrational (excitation) energy at infinite separation. The results for $x < 1$ are taken from Ref. [3].

FIG. 4. Calculated sequence of shapes at time intervals of $10^{-21}$ sec for the symmetric fission of $^{476}184$ and $^{236}U$. The $^{476}184$ nucleus is initially spherical and the $^{236}U$ nucleus is initially at the liquid-drop-model saddle point. Both nuclei initially have 1 MeV of kinetic energy in the fission direction. The viscosity is zero. The shapes are constrained to binary fission in the three-quadratic-surface shape parametrization. The scission configurations are shown dashed.

FIG. 5. Static potential energy of tangent spheroidal fragments calculated in the droplet model as a function of the ratios c/a of their semi-symmetry to semi-transverse axes. The fragments are $^{300}116$ and $^{176}Er$ formed from a $^{238}U + ^{238}U \rightarrow ^{476}184$ parent system.

FIG. 6. Calculated potential energy of tangent spheroidal fragments as a function of the semi-axis ratio c/a of the $^{300}116$ fragment. The elongation of the $^{176}Er$ fragment is held constant at $c/a = 12.6$. The macroscopic contribution to the energy, which is calculated in the droplet model, is given by the dashed line. The total energy, which is obtained by adding shell and pairing corrections for a noninteracting $^{300}116$ nucleus, is given by the solid curve.

FIG. 7. Calculated sequence of shapes at time intervals of $5 \times 10^{-23}$ sec for the fusion of $^{110}Pd + ^{110}Pd$. The energies given are the incident kinetic energy (in the center-of-mass system) of the ions above the liquid-drop-model interaction barrier. The nuclei are tangent spheres at $t = 0$.

FIG. 8. Calculated sequence of shapes at time intervals of $10^{-22}$ sec for the fusion of $^{238}U + ^{238}U$. The energies given are the incident kinetic energy (in the center-of-mass system) of the ions above the liquid-drop-model interaction barrier. The nuclei are tangent spheres at $t = 0$.

FIG. 9. Calculated dynamical paths in the space of center-of-mass separation $r$ and fragment elongation $\sigma$ (defined in Sec. 2) for two colliding $^{150}Nd$ nuclei. The nuclei are initially tangent spheres. The energies labelling the paths give the initial kinetic energy (in the center-of-mass system) above the liquid-drop-model interaction barrier. The terminations of the paths are caused by deficiencies of the shape parametrization.

FIG. 10. Calculated incident kinetic energy (in the center-of-mass system) above the liquid-drop-model interaction barrier necessary for complete fusion as a function of the fissility parameter $x$. The criterion adopted as necessary (but not sufficient) for complete fusion is that the trajectories of the fusing nuclei in the two-dimensional space defined by $r$ and $\sigma$ pass inside the liquid-drop-model saddle point. The center-of-mass coordinate $r$ and the fragment elongation coordinate $\sigma$ are defined in Sec. 2.

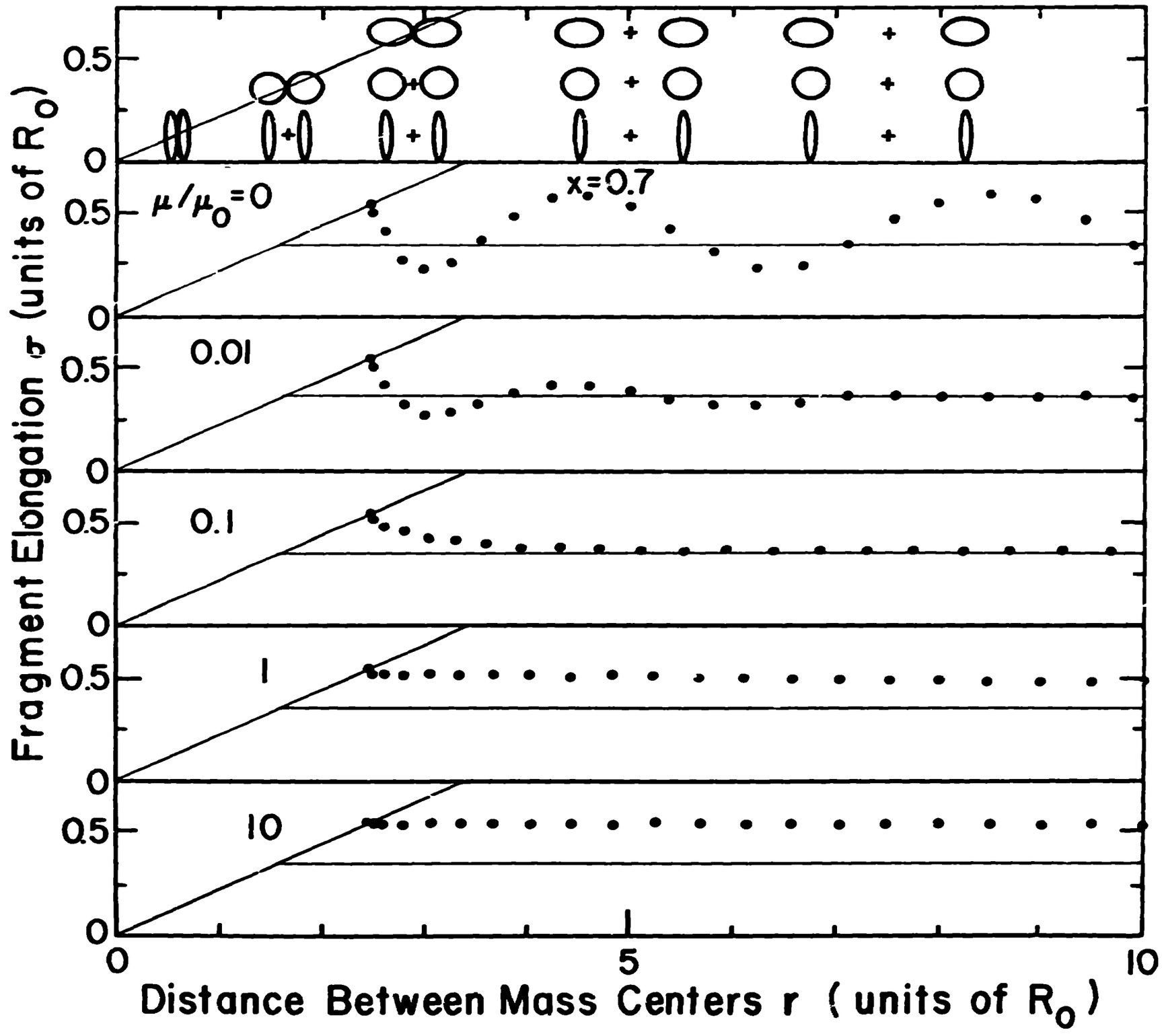
Fragment Elongation σ (units of $R_0$)
$\mu/\mu_0$=0
x=0.7
0.01
0.1
1
10
0.5
0
5
10
Distance Between Mass Centers r (units of $R_0$)

Figure 1

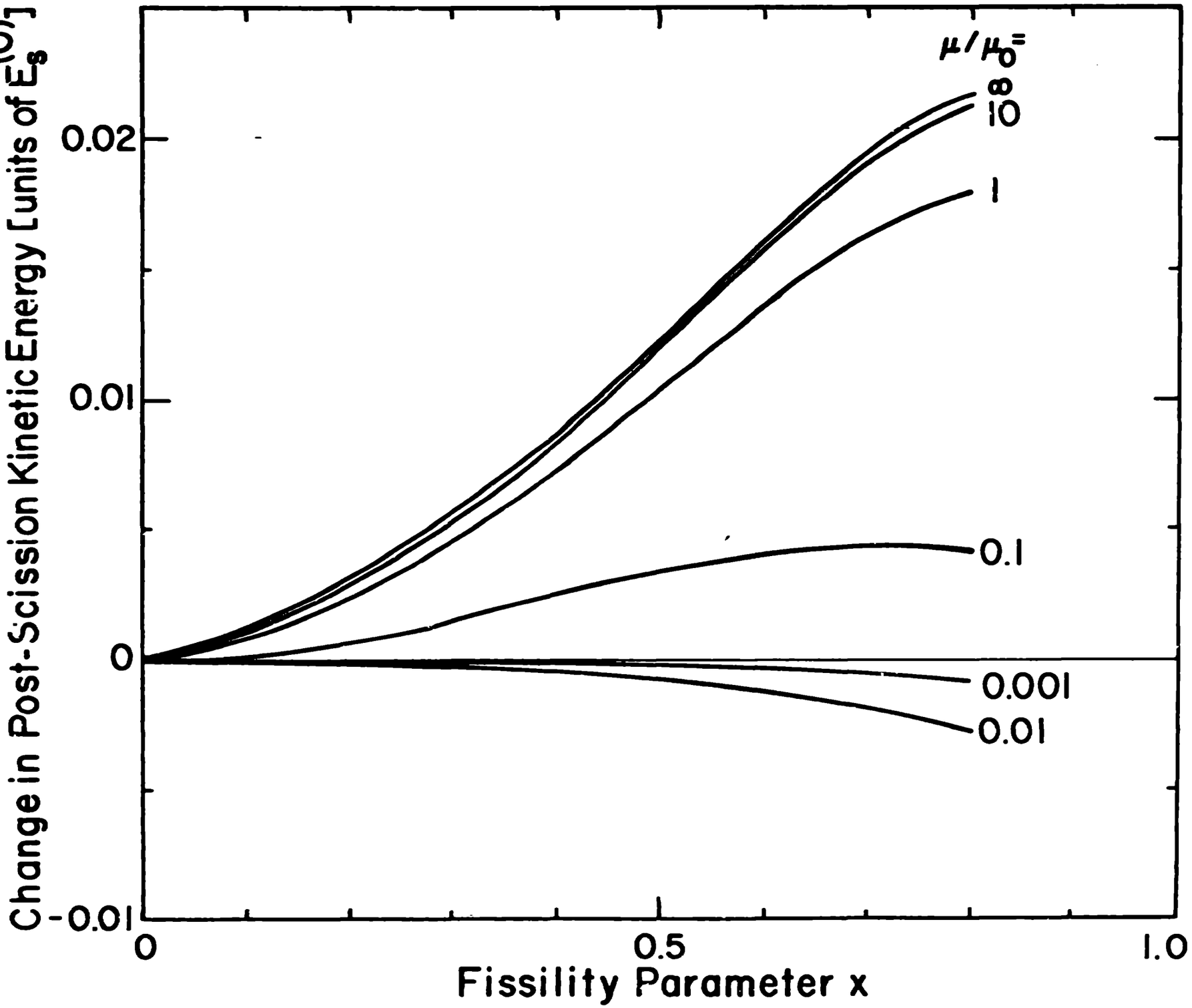
Change in Post-Scission Kinetic Energy [units of $E_s^{(0)}$]
0.02
0.01
0
-0.01
0
0.5
1.0
Fissility Parameter x
$\mu/\mu_0 =$
$10^8$
1
0.1
0.001
0.01

Figure 2

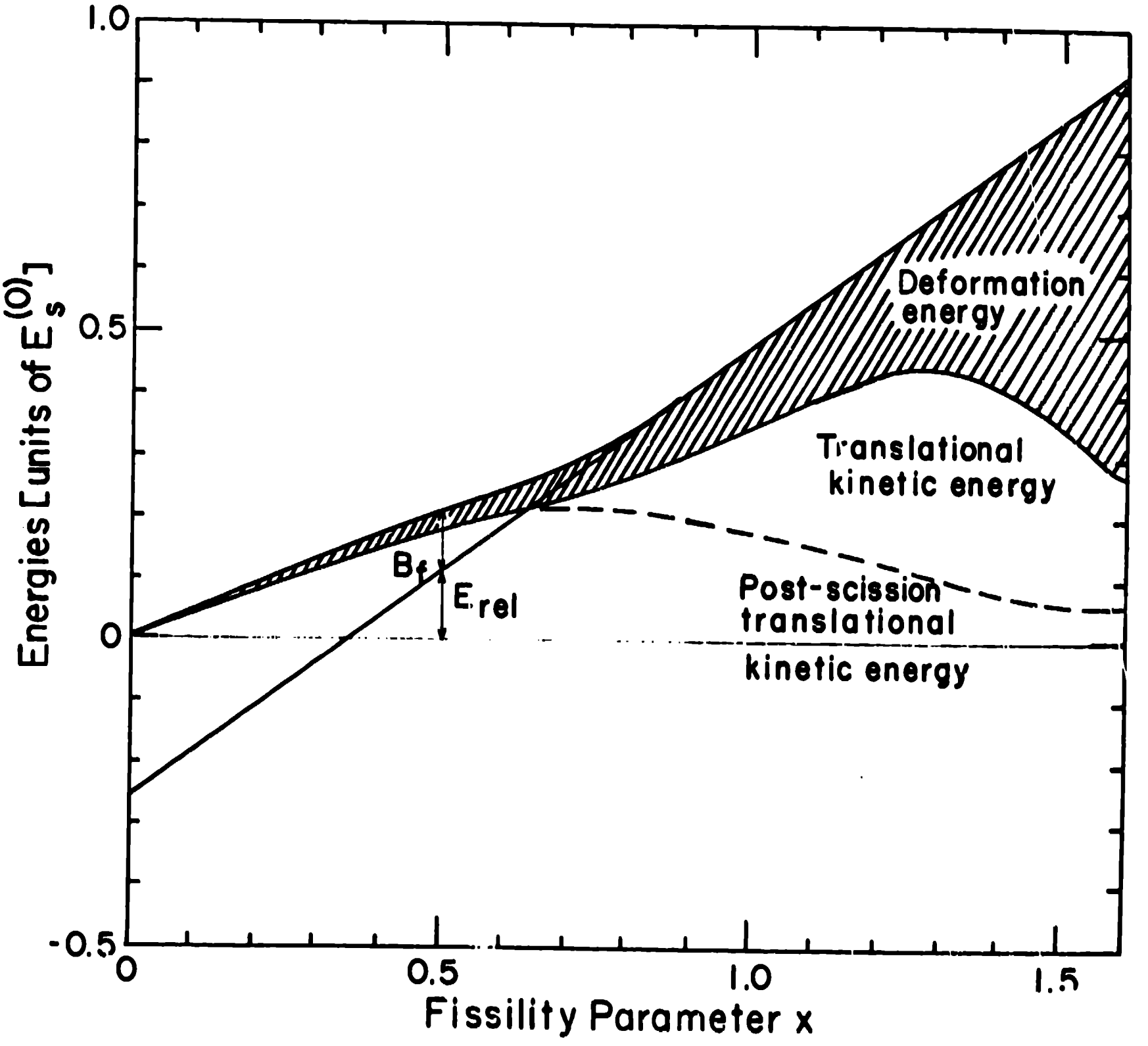
1.0
0.5
0
-0.5
Energies [units of $E_s^{(0)}$]
Deformation energy
Translational kinetic energy
$B_f$
$E_{rel}$
Post-scission translational kinetic energy
0
0.5
1.0
1.5
Fissility Parameter x

Figure 3

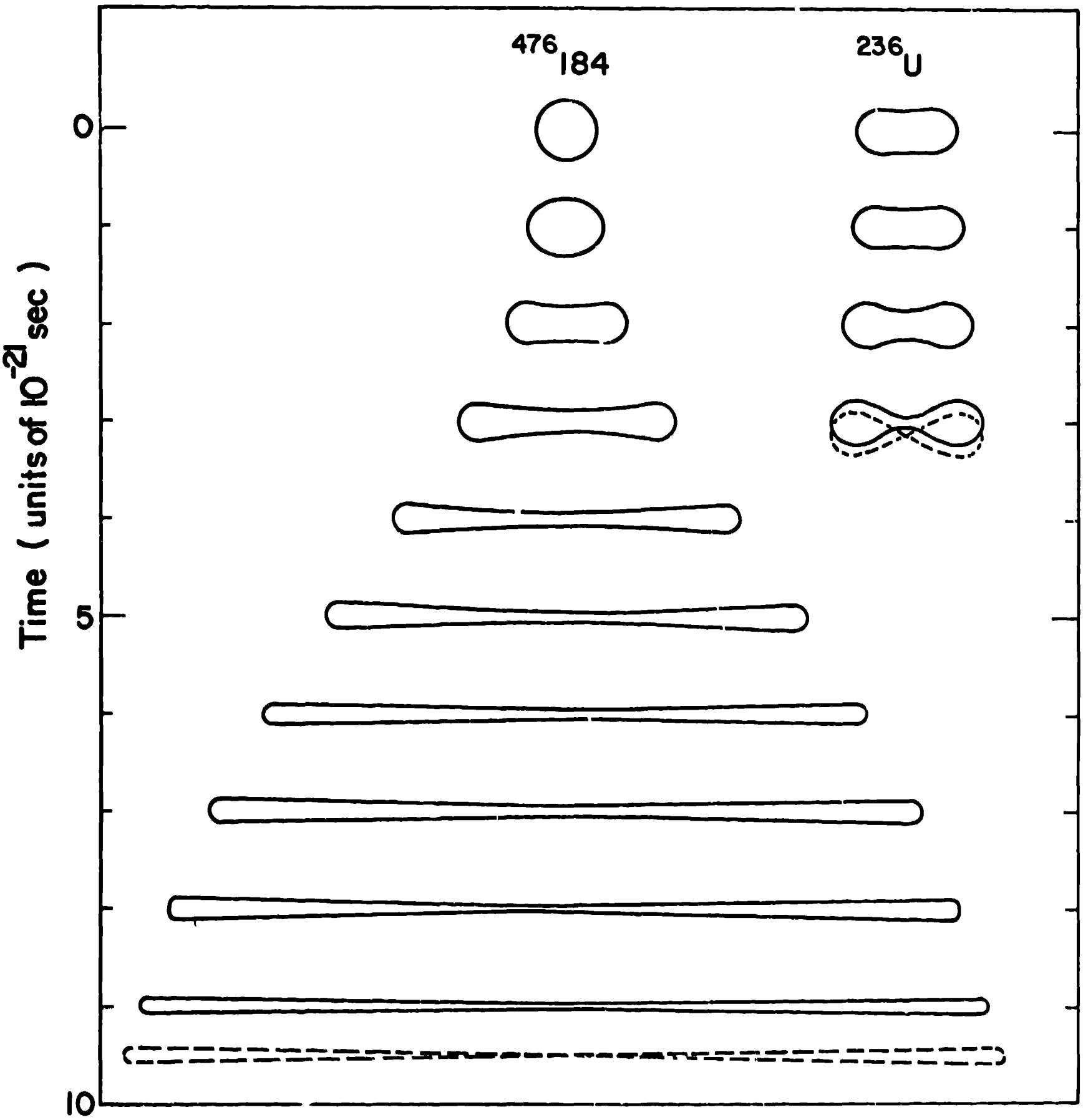


Figura 4

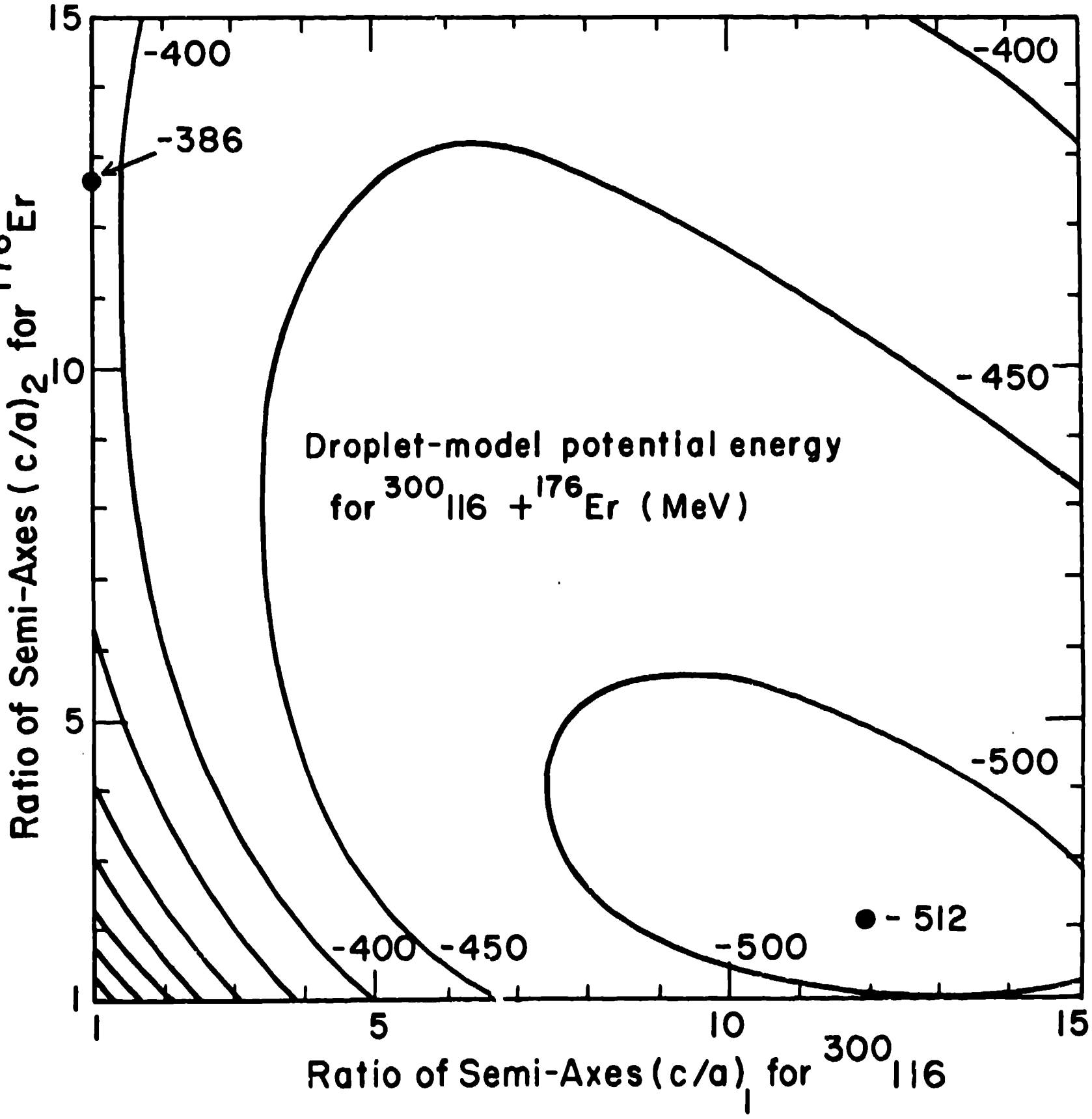
Droplet-model potential energy
for $^{300}_{116}$ + $^{176}$Er (MeV)
-400
-386
-400
-450
-500
-500
-400
-450
-500
● - 512
15
10
5
1
1
5
10
15
Ratio of Semi-Axes (c/a)$_2$ for $^{176}$Er
Ratio of Semi-Axes (c/a)$_1$ for $^{300}_{116}$

Figure 5

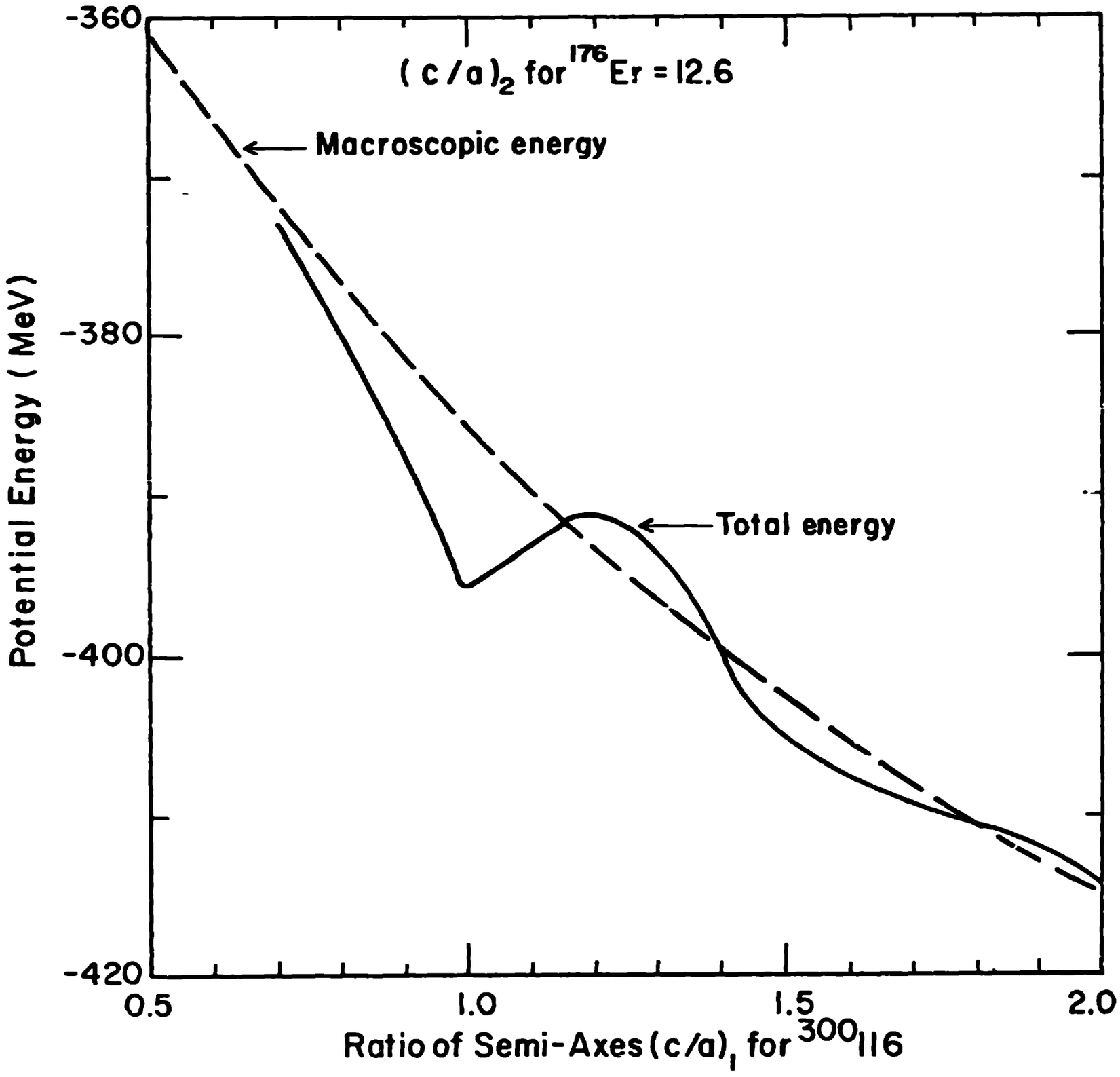
-360
-380
-400
-420
0.5
1.0
1.5
2.0
(c/a)2 for 176Er = 12.6
Macroscopic energy
Total energy
Potential Energy ( MeV)
Ratio of Semi-Axes (c/a)1 for 300116

Figure 6

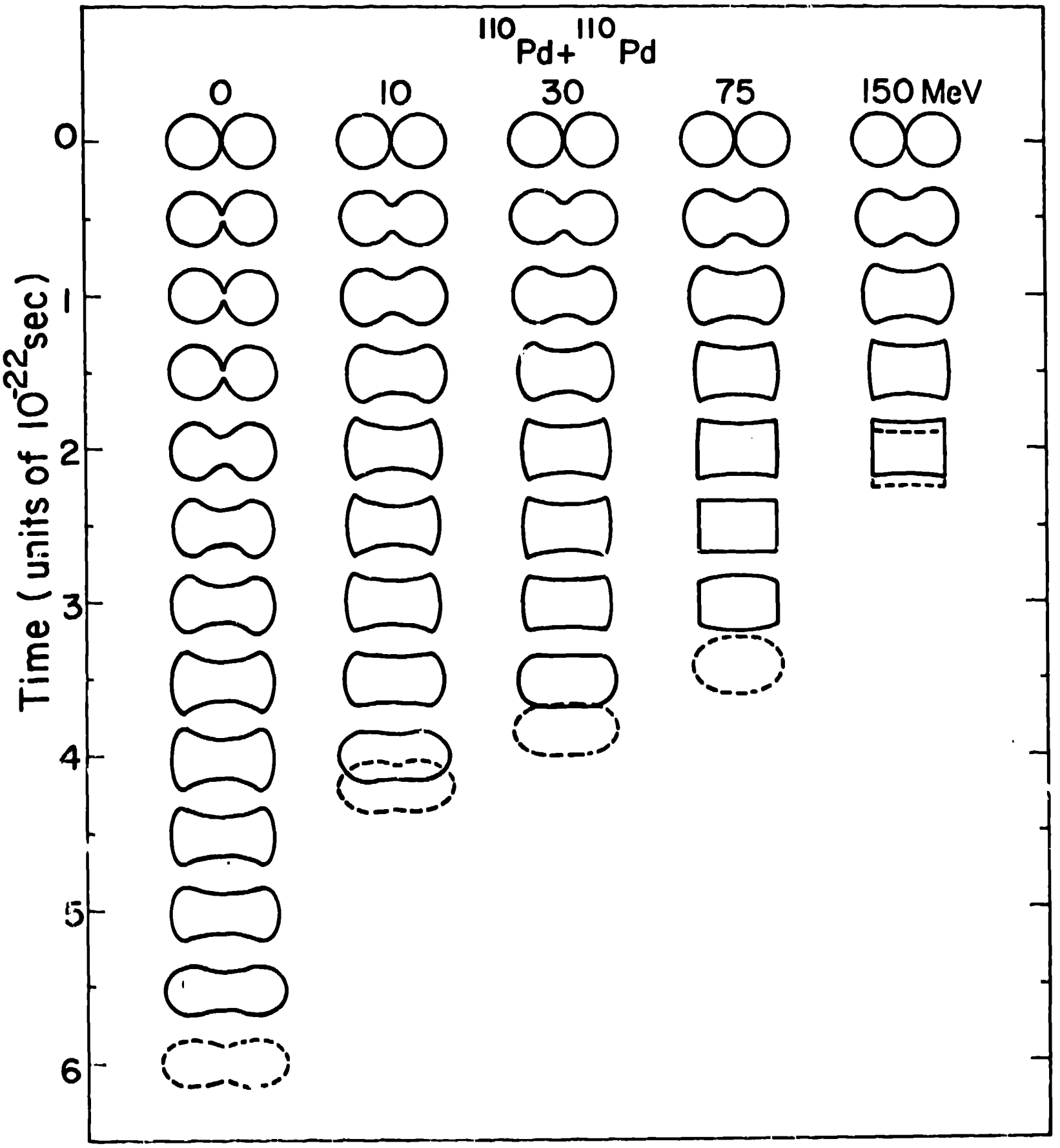


Figure 7

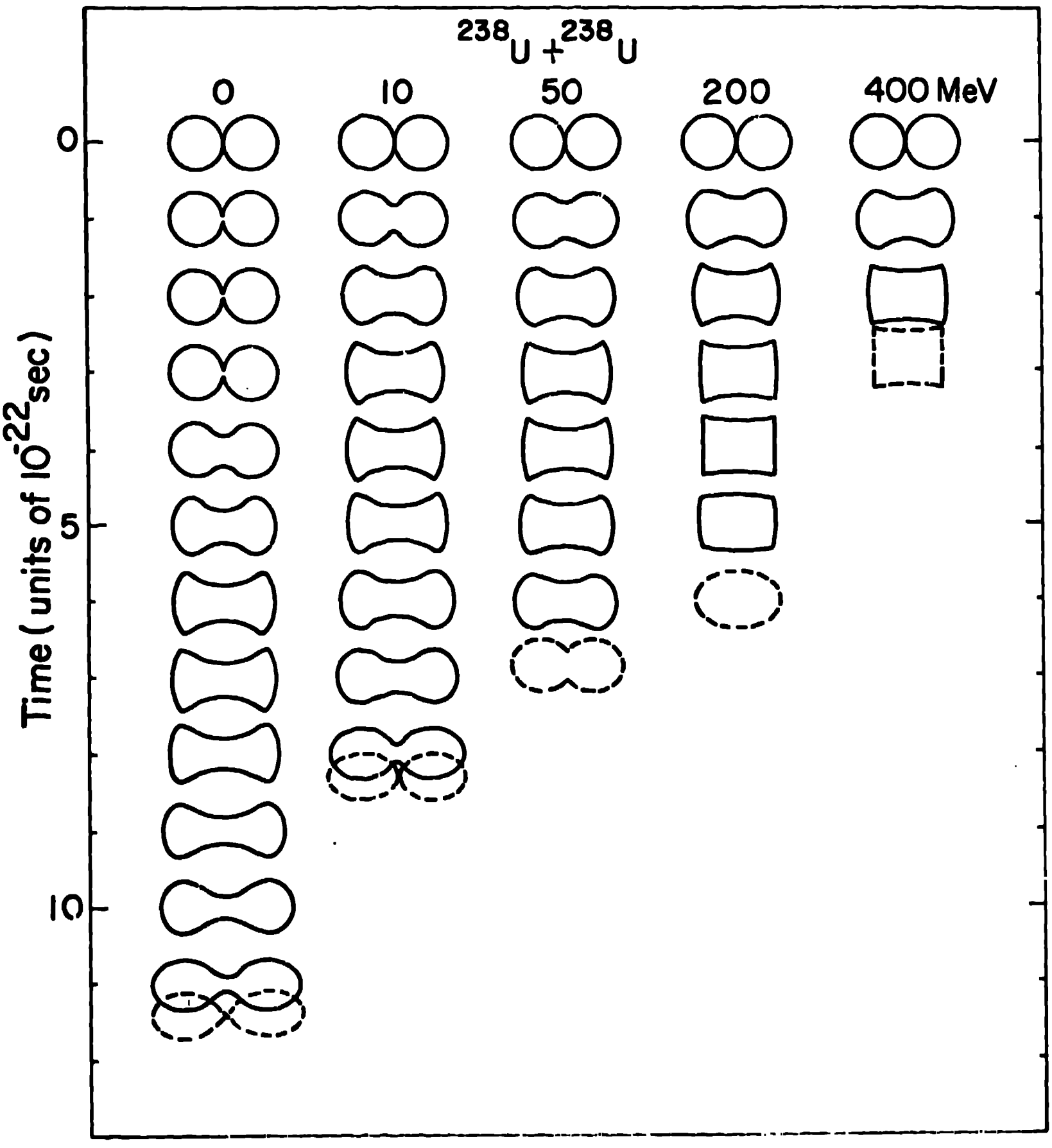


Figure 8

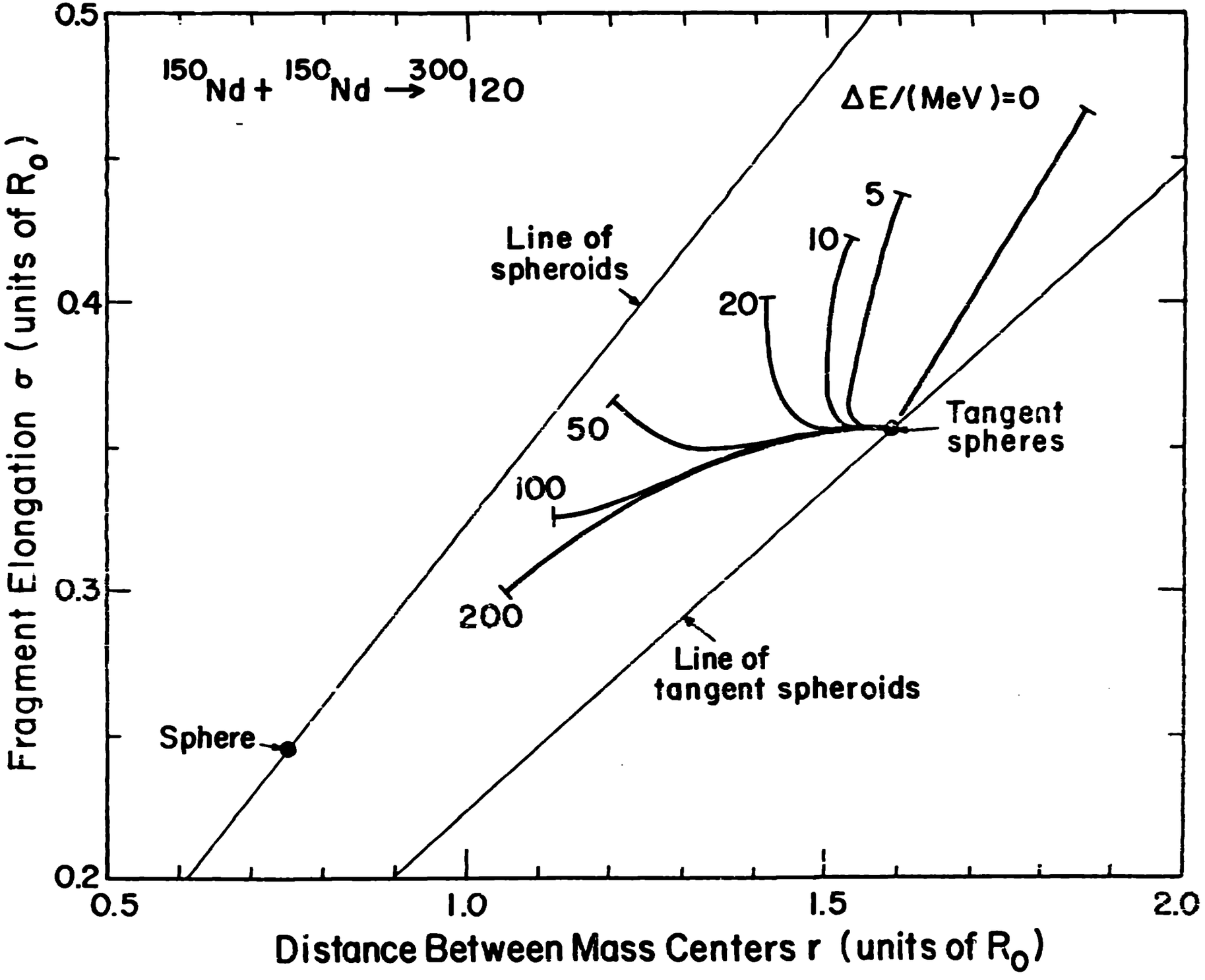
$^{150}Nd + ^{150}Nd \rightarrow ^{300}120$
ΔE/(MeV)=0
5
10
20
50
100
200
Line of spheroids
Tangent spheres
Line of tangent spheroids
Sphere
0.5
0.4
0.3
0.2
0.5
1.0
1.5
2.0
Fragment Elongation σ (units of $R_o$)
Distance Between Mass Centers r (units of $R_o$)

Figure 9

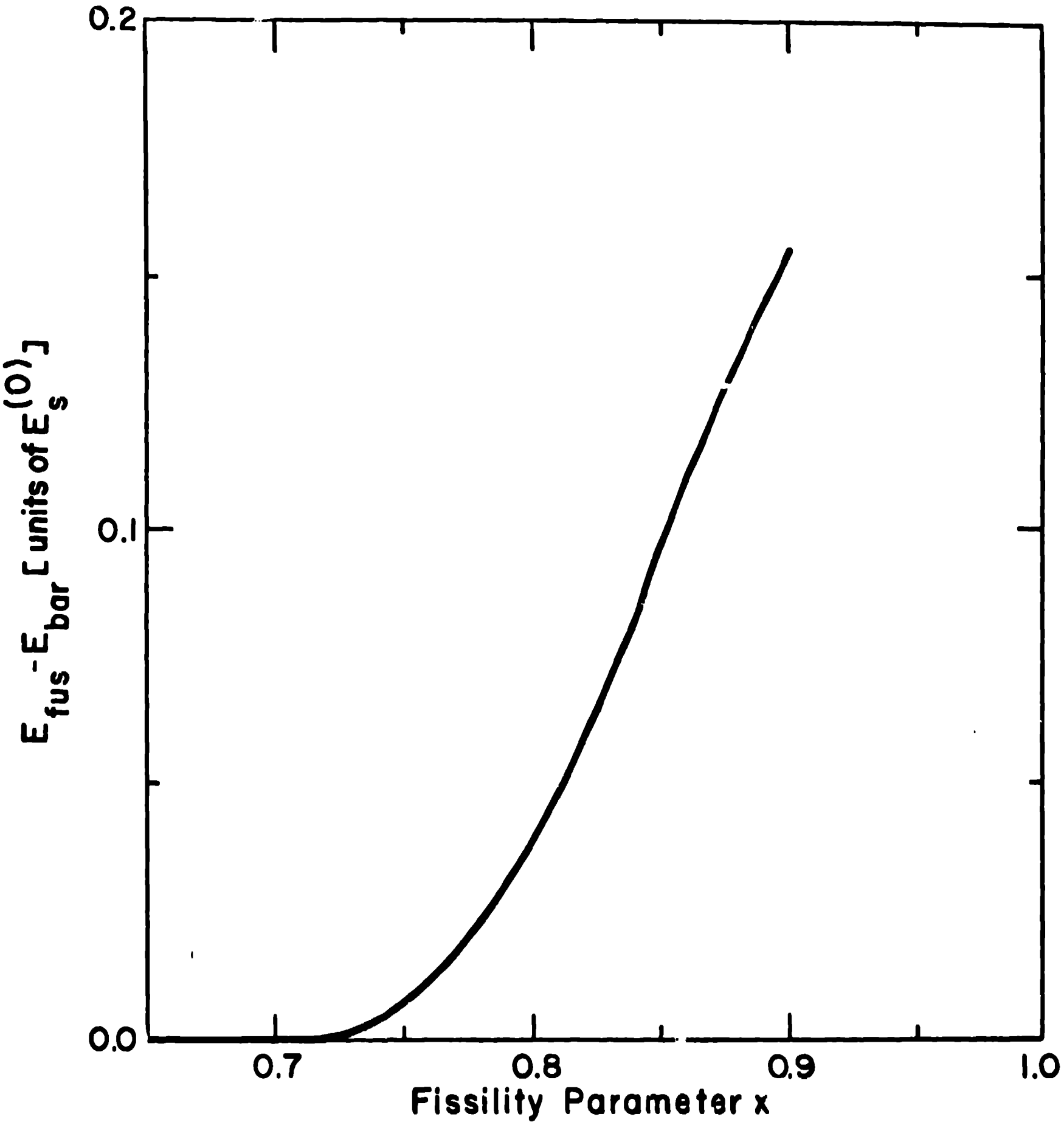
0.2
0.1
0.0
0.7
0.8
0.9
1.0
Fissility Parameter x
$E_{fus}-E_{bar}$ [units of $E_s^{(0)}$]

Figure 10